UNITED STATES DEPARTMENT OF THE INTERIOR

GEOLOGICAL SURVEY

Aeromagnetic measurements in the Cascade Range and Modoc Plateau of northern California --- Report on work done from December 1, 1980, to May 31, 1981

By Richard Couch and Michael Gemperle

Oregon State University
Corvallis, Oregon 97331

Open-File Report 82-933

1982

xxxxxxxxxxxxxxxxxxxxxxxxxxxxxxxxxxxxxxxxxxxxxxxxxxxxxxxxxxxxxxxxxxxxxxxxxxxxxxxxxxxxxxx

Project Information

This report was prepared under Grant No. 14-08-0001-G-623 to Oregon State University from the U.S. Geological Survey's Geothermal Research Program, with Dr. Richard Couch of the School of Oceanography as the Principal Investigator. The period of the grant was from June 1, 1979, to October 31, 1981. Objectives of the grant were as follows: to obtain high-quality aeromagnetic data over a 30,000-square-kilometer area in the Cascades and Modoc Plateau of northern California and (2) to analyze the data in terms of structure, volcanic centers, regional trends, Curie-temperature isotherm depths, and the implications concerning the geothermal energy potential of the area. The data obtained during the course of this project and described in this report are on file in the National Geophysical Data Center (NGDC) of NOAA in Boulder, CO.

TABLE OF CONTENTS

Figures

Table

Abstract

Spectral analysis of aeromagnetic data collected over north-central California during the summer of 1980 aided in determining magnetic-source bottom depths beneath the survey area. Five regions of shallow magnetic source bottom depths were detected: 1) Secret Spring Mountain and National Lava Beds Monument area, 2) the Mount Shasta area, 3) the Eddys Mountain area, 4) the Big Valley Mountains area, and 5) an area northeast of Lassen Peak. Except for the Eddys Mountain area, all regions exhibiting shallow depths are suggested to be due to elevated Curie-point isotherms.

The elevated Curie-point depth beneath Secret Spring Mountain and the National Lava Beds Monument area was found to be 4-7 km BSL (Below Sea Level) and is an extension of a zone mapped beneath an area immediately to the north in Oregon. A similar depth was detected for the Mount Shasta area and the area northeast of Lassen Peak. A depth of 4-6 km BSL was detected beneath the Big Valley Mountains area. The shallow Curie-point depths beneath Secret Spring Mountain, Mount Shasta, Big Valley Mountains, and the area northeast of Lassen Peak appear to form a segmented zone of elevated Curie-point isotherm depths which underlies the High Cascade Mountains and Modoc Plateau in north-central California. A small area of shallow depths to magnetic-source bottoms, 4-5 km BSL, beneath the Eddys Mountain area is attributed to a lithologic boundary rather than an elevated Curie-point isotherm.

Deeper magnetic source bottom depths were mapped throughout the remainder of the study area, with depths greater than 9 km BSL indicated beneath Lassen Peak and greater than 11 km BSL indicated beneath the Western Cascades, Eastern Klamath Mountains, and Great Valley.

Research Objective

Figure 1 outlines an area of approximately 30,000 square kilometers that extends from the Oregon-California border at 42°N. latitude to south of Lassen Pk. at 40°15'N. latitude and approximately between 120°45' and 122°45'W. longitude. This area encompasses the southern Cascade Range, the adjoining Modoc Plateau including the Medicine Lake Highlands, the northern terminus of the Great Valley, and the easternmost flank of the Klamath Mountains. The objectives of this study are: to obtain precise aeromagnetic measurements in the region outlined in Figure 1; to delineate the magnetic anomalies associated with the Cascade Range and the transition region between the Cascade Range and the basin and range structures east of the Cascades; to determine the depths to the magnetic sources; and to estimate the depths of the Curie-point isotherm in the region. These data and analyses will assist in the geologic and structural interpretation of the region and provide information to help assess the geothermal resource potential of the region.

U.S. Geological Survey Open-File Report 82-932 (Couch and Gemperle, 1982) describes and depicts the aeromagnetic anomalies mapped in northern California in the earlier phases of this study. This report outlines the method of analysis of the observed anomalies, lists the estimated depths to the Curie-point isotherm in the area, and presents a map of the estimated depth to the Curie-point isotherm and/or the depth to the bottom of the magnetic anomaly-sources.

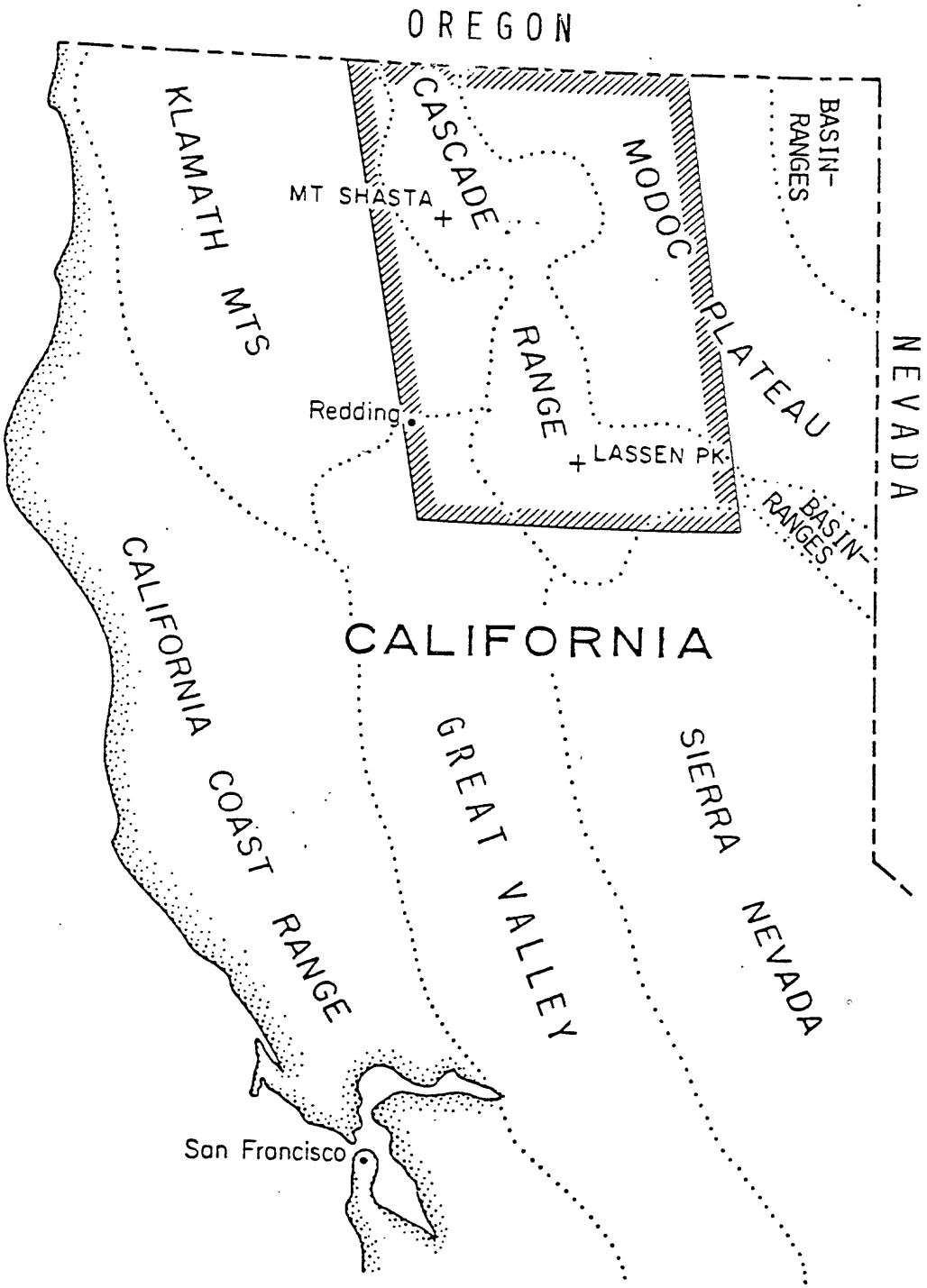

Figure 1. Northern California physiographic provinces and aeromagnetic survey location (outlined by shading).

The objectives, (1) to determine the depths to magnetic sources and (2) to estimate the depths to the Curie-point isotherm for the region outlined in Figure 1, have been addressed, and the results are summarized in this report. In addition, data are presented that will aid in assessing the geothermal resource potential of this area.

Method of Analysis

To obtain the estimated depth of the bottom of the magnetic-anomaly sources, the magnetic anomalies were examined in terms of their wavelengths or spacial frequencies according to a type of spectral analysis employed by Spector (1968), Spector and Grant (1970), Smith et al. (1974), Boler (1978), Connard (1979), and McLain (1981). The present treatment of the theoretical formulations is only briefly outlined below.

The magnetic-anomaly map is converted to spacial frequencies using a discrete form of a 2-D Fourier transform (DFT). The Fourier transform (FT) for a model consisting of magnetized rectangular boxes with horizontal tops and bottoms can be written in closed form and is given by Bhattacharyya (1966) as

$$F(u,v) = 2\pi \cdot M \cdot e^{-h(u^2+v^2)^{1/2}} \cdot (1-e^{-t(u^2+v^2)^{1/2}}) \cdot S(u,v) \cdot R_p(u,v) \cdot R_g(u,v)$$

Where M = magnetic moment/unit depth

h = depth to the top of the prism

t = thickness of the prism

S = shape factor for horizontal size of the prism

R_p = factor for magnetization direction of the prism

R_g = factor for geomagnetic field direction

u,v = spatial frequencies in radians/unit distance in the x and y directions respectively.

Spector (1968) considered the square of the amplitude of $F(u,v)$, defined as the energy spectrum, $E(u,v)$. When transcribed into polar wavenumber coordinates in the u,v frequency plane, the energy spectrum becomes

$$E(r,\theta) = 4\pi^2 \cdot M^2 \cdot e^{-2hr} \cdot (1-e^{-tr})^2 \cdot S^2(r,\theta) \cdot R_p^{\,2}(\theta) \cdot R_g^{\,2}(\theta)$$

where $r = (u^2+v^2)^{1/2}$ and $\theta = \tan^{-1}(u,v)$.

Spector and Grant (1970), regarding $E(u,v)$ from a statistical sense, introduced the idea of modelling magnetic layers as an ensemble of prisms. Each point in ensemble space corresponds to a prism with a particular set of parameter (width, length, thickness, etc.) values. They next assumed they could equate the ensemble average of E denoted by $\langle E \rangle$ to the expected value of E. The equation for $\langle E \rangle$ is then

$$\langle E(r,\theta) \rangle = 4\pi^2 \cdot \bar{M}^2 \cdot \langle R_g^{\,2}(\theta) \rangle \cdot \langle R_p^{\,2}(\theta) \rangle \cdot \langle e^{-2hr} \rangle \cdot \langle (1-e^{-tr})^2 \rangle \cdot \langle S^2(r,\theta) \rangle .$$

They argue this equation can be simplified by dividing out the $\langle R_g^{\,2}(\theta) \rangle$ and $\langle R_p^{\,2}(\theta) \rangle$ factors in a 'rotation-to-the-pole' operation which gives

$$\langle E(r,\theta) \rangle = 4\pi^2 \cdot \bar{M}^2 \cdot \langle e^{-2hr} \rangle \cdot \langle (1-e^{-tr})^2 \rangle \cdot \langle S^2(r,\theta) \rangle .$$

The simplification is valid if the geomagnetic field direction does not vary appreciably over the survey region and if this direction differs little from that in the crustal magnetic sources. The change in the anomaly pattern effected by a 'rotation-to-the-pole' is less for survey regions located at high magnetic latitude with 'normal' looking anomalies.

Finally an average with respect to θ is taken to give:

$$\left\langle \bar{E}(r) \right\rangle = 4\pi^2 \cdot \bar{M}^2 \cdot \left\langle e^{-2hr} \right\rangle \cdot \left\langle (1-e^{-tr})^2 \right\rangle \cdot \left\langle \bar{S}^2(r) \right\rangle$$

where $\bar{E}$ and $\bar{S}$ indicate the average over θ.

Spector and Grant (1970) state that the term $\left\langle e^{-2hr} \right\rangle$, which Spector (1968) showed to have the value $e^{-2\bar{h}r}$ for $\Delta h/\bar{h} < .25$, and $r < 1/\bar{h}$, is the dominant factor in determining the decay of the spectrum. Clearly then, mean depths to sources, $\bar{h}$, are proportional to the slope of the natural logarithm of $\left\langle E \right\rangle$.

To determine d, the depth to the bottom of the ensemble, Spector and Grant (1970) show that the combined effect of factors $\left\langle (1-e^{-tr})^2 \right\rangle$ and $\left\langle e^{-2hr} \right\rangle$ is to introduce a peak in the spectrum which shifts towards longer wavelengths as the value of t increases. Maximizing $\left\langle (1-e^{-tr})^2 \right\rangle \cdot \left\langle e^{-2hr} \right\rangle$ with respect to r, the resulting equation can be solved for d and becomes

$$\bar{d} = \frac{\bar{t}}{1-\exp(-\bar{t}r_{max})}$$

where the bars indicate mean values for the ensemble parameters. The dependence of $\bar{d}$ on $\bar{t}$ adds further uncertainty to depth-to-bottom calculations. Although $d \to \frac{1}{r_{max}}$ as $t \to o$ for laminar bodies, such thin bodies

require unreasonably large values of magnetization. Shuey et al. (1977) suggest a minimum source body thickness of 5 km, a constraint used in this study. Thus the source-bottom is being resolved and its depth may be determined when a peak occurs in the energy spectrum.

Because the magnetic-source bottom is associated with the lower frequencies, it is better sampled when the area of the survey map is larger. However a larger mapped area gives a more regional calculation for the depth-to-magnetic-source bottom and this reduces the ability to observe the possible occurrence of basement undulations. The depth to which the sampled area or window can see is also dependent on its size (L by L). If the magnetic bodies extend much deeper than L/2 , the highest frequency associated with their bottom depths becomes smaller than the lowest frequency the window is capable of sampling, i.e. its fundamental frequency. It should be noted that Spector (1968) sets the maximum depth to which a window of size L by L can see as L/4.

Lastly there is the effect on the energy spectrum by the shape factor, S, given by Spector and Grant (1970) as:

$$S(r,\theta) = \frac{\sin (a \cdot r \cdot \cos \theta)}{a \cdot r \cdot \cos \theta} \cdot \frac{\sin (b \cdot r \cdot \cos \theta)}{b \cdot r \cdot \cos \theta}$$

As the horizontal dimensions, 2a and 2b, increase, the short-wavelength side of the spectrum is depressed which causes a slight movement of the spectral peak towards longer wavelengths. Shuey et al. (1977) show that the effect of a body with horizontal dimensions comparable to the survey area is to displace the spectral maximum to zero frequency. To remove this effect, which is equivalent to removing a regional anomaly gradient, the anomalies are detrended before computing the spectrum

(Connard, 1979). This process involved subtracting a plane surface fitted to the gridded data by least squares. Such detrending ensures greater power in the fundamental frequency as opposed to the zero frequency. Hence, for spectral plots analyzed in this study, those with a one-point maximum occurring at the fundamental frequency indicate that source bottoms are not being resolved.

Details of Computer Processing

Conversion of the aeromagnetic anomalies into a spacial frequency domain is accomplished by (1) gridding, (2) detrending, (3) tapering, and (4) applying a two-dimensional Fourier transform to the data. Programs used in this procedure are documented in Boler (1978), Pitts (1979), Connard (1979), McLain (1981), and Couch and Gemperle (1982).

To interpolate the flight line data onto an equally spaced grid, an algorithm by Briggs (1975) was used which minimizes the curvature of a surface through the value at each grid point. The grid spacing was set at .285 km in both X(E-W) and Y(N-S) directions. Although this spacing is larger than the average data spacing of 0.13 km, it is sufficient to avoid aliasing problems and follows Spector's (1968) suggestion that Δx and Δy should be no greater than one-quarter the width of the sharpest magnetic feature on the anomaly map. At this spacing, the anomaly map is converted to a single grid 594 x 681 in size. The boundaries of the grid relative to the flight line data are shown in Figure 2.

At this point subgrids representing parts of the survey area can be extracted. For any grid selected, a least squares fitted plane is subtracted from the grid. This detrending removes any remaining regional field from the data.

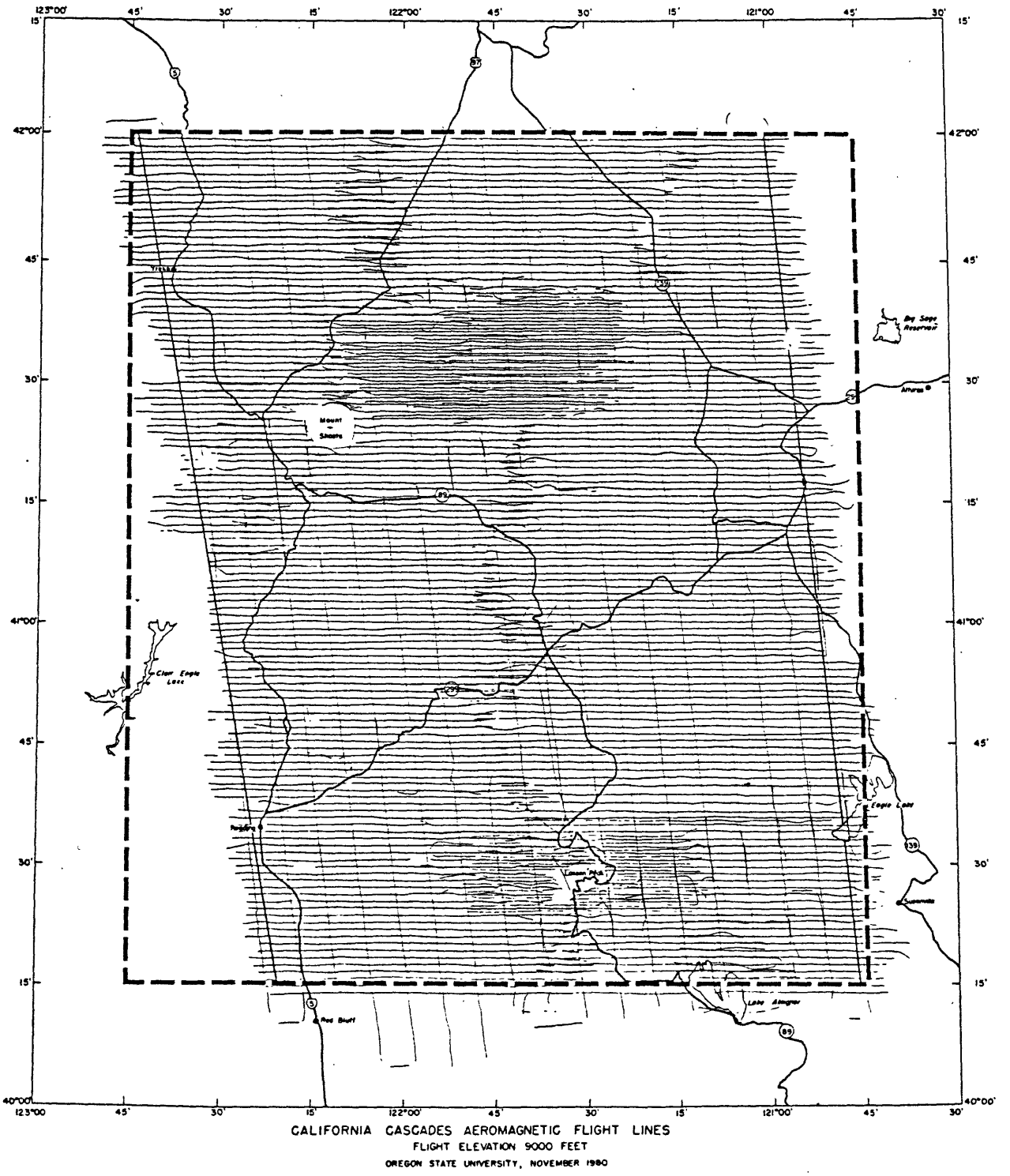

Figure 2. Boundaries of the 594 by 681 main grid.

Before the Fourier transform can be applied, the grid must also be tapered at the edges to make the data periodic. In the frequency domain, sharp edges of the window or grid cause large amounts of distortion at frequencies higher than 4π/width of the survey area (Spector, 1968). This study minimizes these edge effects by applying a cosine-squared window to strips 10 points wide which comprise the subgrid's boundaries.

The computer algorithm to do the discrete Fourier transform is from Rob Clayton at Stanford University (personal communication). It is a two-dimensional fast Fourier transform and requires equally spaced data on a square grid with 2" x 2" points on a side. Subgrids of size 512 x 512 (146 km x 146 km), 256 x 256 (73 km x 73 km), and 128 x 128 (36 km x 36 km) were transformed for study.

Each subgrid was then rotated to the pole by multiplying transformed data by the appropriate factors. Magnetization directions for geomagnetic field and magnetic bodies of 65° inclination and 18.87° declination were rotated to the vertical with a resulting 90° inclination and 0° declination. The program used is documented in Boler (1978).

For the purpose of magnetic source-bottom depth determinations in the present study area, the radial average of the natural logarithm of the energy spectrum of 217 subgrids was computed. An example of such a spectral plot is shown in Figure 3. A radial average is computed by averaging the squared amplitude or energy of each element (m,n) of the complex two-dimensional frequency domain array generated by the Fourier transformation. Each point on the spectral plot represents the average of all elements within a ring Δf ($\Delta r/2\pi$) wide. Discrete sampling allows only multiple values of Δf ($m\Delta f$ or $n\Delta f$ where m, n = 0,1,2,....). This means, for example, that the 8 elements with $0.5<(m^2+n^2)^{1/2} \leq 1.5$ are averaged

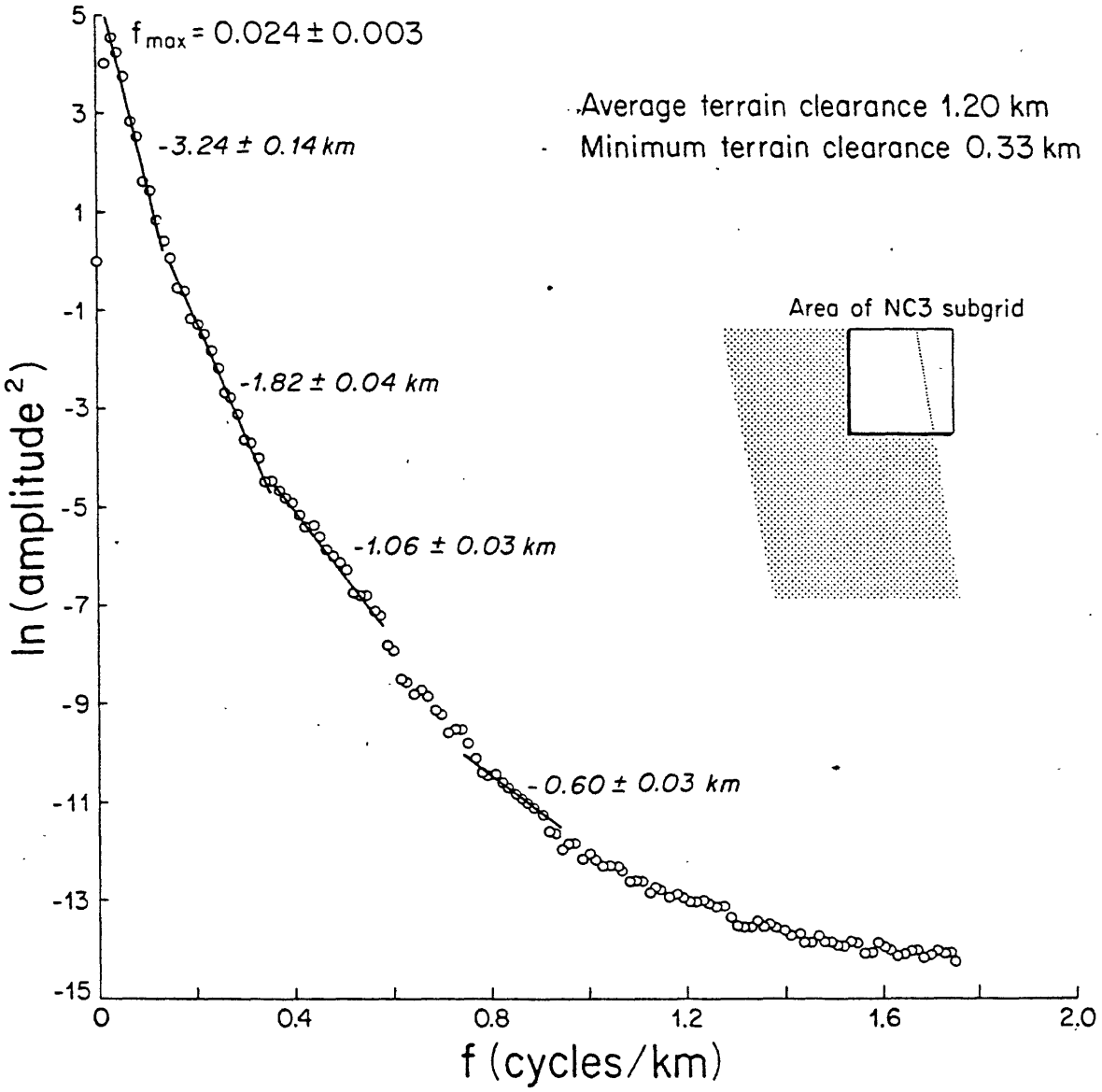

Figure 3. Radially averaged spectrum of the northeastern corner (NC3 subgrid, 256 x 256 points) of the northern California aeromagnetic data.

for the second point on the plot. The exception is the zero frequency element (m = 0, n = 0) which is the first point plotted. This element is not averaged with any other.

Mean depth-to-source-top or h determinations are made by fitting a least-squares line to the points on the spectral plots. Recall that the slope of this line is proportional to h. Errors in slope as indicated on the plot of Figure 3 represent uncertainties in a straight-line fit to the curve and are not a measure of the accuracy of the source depths themselves.

Magnetic-Source Depth Determinations from Spectral Analysis

A magnetic source body may be depth limited in two ways. First, the magnetic-source bottom may represent a lithologic boundary between magnetic and non-magnetic material. Source bodies depth-limited in this manner include sills intruded into sedimentary layers and volcanic flows overlying non-magnetic volcaniclastic material.

Second, the magnetic basement may represent the depth at which rocks lose their ferromagnetic properties due to high temperatures. Such a depth is referred to as the Curie-point isotherm depth. A steep vertical temperature gradient is implied in areas which exhibit geothermal surface manifestations such as recent volcanism, high heat flow, and hot springs, and the magnetic-source-bottom depth is often interpreted as the Curie-point isotherm depth.

Assuming the Curie-point isotherm depth interpretation to apply, values for vertical temperature gradients and heat flow were calculated for regions exhibiting similar magnetic-source depths. Because these values appear reasonable and because much of the study area displays recent

volcanism and current hydrothermal activity, the Curie-point depth-limited interpretation may be valid for the region.

Two 512 x 512 (146 km x 146 km) subgrids of the 594 x 681 (169 km x 194 km) main grid were processed to produce spectral plots. The two grids overlap each other by about 2/3 their N-S extent. The south grid indicated the possibility of magnetic-source-bottom depths shallow enough to be discerned by a smaller grid size or "window". The north grid did not. Even so, the entire survey area was initially subdivided into twelve 256 x 256 (73 km x 73 km) grids, and spectral plots produced. These subgrids were overlapped to increase resolution. As an example, the radially averaged spectral plot of grid No. 3 is shown in Figure 3. The corresponding calculated magnetic-source depth range is shown in Figure 4.

In three cases, peaks occurred in the spectral plots of the 256 x 256 subgrids indicating bottom source depths were being resolved. Because two of these peaks were "noisy", the grids were shifted by varying amounts in an attempt to sharpen the peaks. An additional subgrid was centered over the Medicine Lake Highlands, an area of current interest. Therefore a sum total of seventeen 256 x 256 spectral plots were produced.

The occurrence of peaks in the 256 x 256 spectral plots suggest shallower depths might be observed using a smaller subgrid or "window". Hence, a grid size of 128 x 128 points or 36 km x 36 km was used to sweep across the survey area in an overlapping manner referred to as a "moving window" technique. Distances between centers of adjacent windows vary. For the most part, a minimum separation between centers of 32 grid-space units, or 1/4 the dimension of the window, was used. Although a smaller separation was used at locations where clarification was sought.

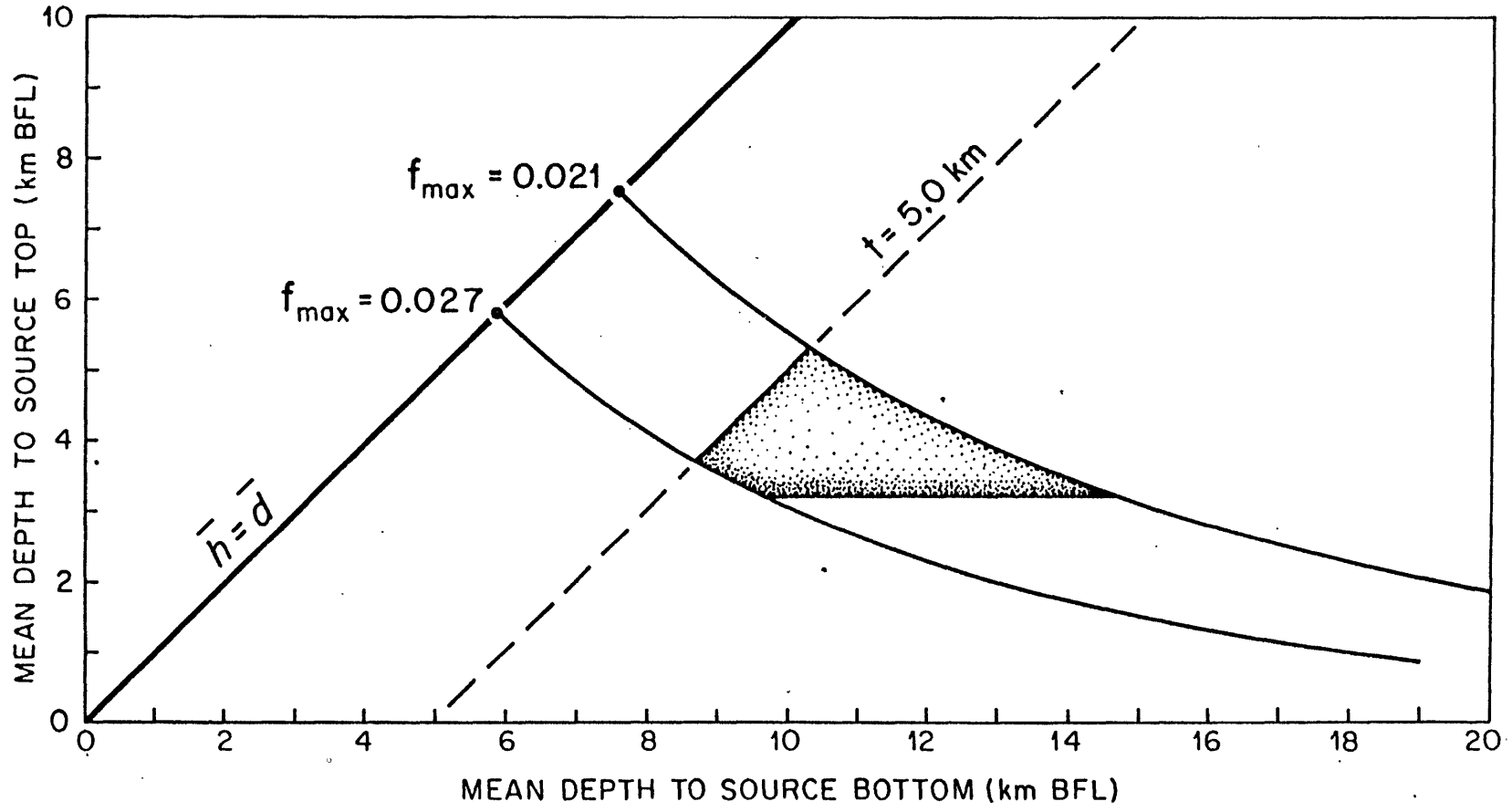

Figure 4. Estimated limits of Curie-point and/or magnetic-source depths for NC3 subgrid in the extreme northeast corner of northern California survey area.
(BFL - below flight level)

A total of 198 128 x 128 spectral plots were produced for analysis. As a result of the "moving window" technique, several regions of shallow magnetic-source basements which might be interpreted as shallow Curie-point depths were mapped. These areas are: (1) the Secret Spring Mountain and Lava Beds National Monument areas, (2) the Mount Shasta area, (3) the Mount Eddy area, (4) the Big Valley Mountains area, and (5) an area northeast of Lassen Peak.

The area starting from Secret Spring Mountain on the Oregon - California border and extending across Lava Beds National Monument was outlined with thirty 128 x 128 subgrids. Ten of these thirty spectral plots resolved a magnetic-source bottom and exhibited spectral peaks between .033 and .053 cycles/km. In calculating the Curie-point isotherm depth, the depth to the top of the deepest discernable source, $\bar{h}$, is required. For those spectral plots exhibiting peaks, the determined source-depth values varied over a wide range. The mean source depth of the ten spectral plots was $2.7 \pm .6$ km BFL (Below Flight Level).

The Mount Shasta area was outlined with twenty-six 128 x 128 subgrids. Eight of these twenty-six spectral plots resolved a magnetic-source bottom and exhibited spectral peaks between .033 and .053 cycles/km. In calculating the Curie-point-depth, the depth to the top of the deepest discernable source, $\bar{h}$ is required. Six of the eight spectral plots exhibiting spectral peaks indicated no discernable source depths deeper than $1.9 \pm .1$ km BFL. The remaining two of the eight spectral plots containing peaks and representing subgrids centered along the eastern boundary of the Mount Shasta area indicated source depths of 2.27 and 2.39 km BFL.

Eight 128 x 128 subgrids were used to outline the region south of Mount Eddy in the Eddys Mountain Range. Two of these eight spectral

plots resolved a magnetic-source bottom and exhibited peaks between .034 and .048 cycles/km. In calculating the Curie-point-depth, the depth to the top of the deepest discernable source, $\bar{h}$, is required. The two spectral plots exhibiting peaks indicated source depths of 2.40 and 2.52 km BFL.

The Big Valley Mountains area was outlined with thirty-nine 128 x 128 subgrids. Seventeen of these thirty-nine spectral plots resolved a magnetic-source bottom and exhibited spectral peaks between .035 and .055 cycles/km. In calculating the Curie-point-depth, the depth to the top of the deepest discernable source, $\bar{h}$, is required. Source depths determined for these seventeen spectral plots varied somewhat and gave an average value of $2.3 \pm .3$ km BFL.

Thirty-four 128 x 128 subgrids were used to outline the region north/north east of the Lassen Peak area. Fifteen of these thirty-four spectral plots resolved a magnetic-source bottom and exhibited peaks between .033 and .055 cycles/km. In calculating the Curie-point depth, the depth to the top of the deepest discernable source, $\bar{h}$, is required. For those spectral plots exhibiting peaks, the determined source-depth values varied somewhat. Fourteen of the fifteen spectral plots exhibiting peaks indicated a mean source depth of $1.9 \pm .2$ km BFL. The remaining plot containing a peak and representing a subgrid centered at the extreme northeast corner of the Lassen Peak area indicated a source depth of 2.72 km BFL.

Additional 128 x 128 subgrids were centered at various points throughout the main (594 x 681) grid. None of the spectral plots from these subgrids exhibited spectral peaks, thereby indicating that the Curie-point depth beneath these areas was deeper than the depth a

128 x 128 subgrid can adequately resolve, or about 9 km BFL.

Table 1 summarizes the magnetic-source-bottom depths estimated from the frequencies associated with the spectral peaks. Minimum depth-to-bottom estimates given in the table were calculated using the 5-km minimum magnetic-source thickness discussed earlier. Maximum depth-to-bottom estimates given in the table result in part from using the depth-to-source-top estimates derived from spectral plots containing peaks. Those grids included in the summary are the two 512 x 512 subgrids, the seventeen 256 x 256 subgrids, and the 128 x 128 subgrids mentioned above.

The table also includes geothermal gradients and average heat-flow values where it is assumed that the magnetic-source-bottom depth is equivalent to the depth to the Curie-point isotherm. Two possible Curie-point temperatures of 300°C and 580°C were assumed to calculate the geothermal gradients. Average heat-flow values were calculated assuming a conductivity value of 1.7 $Wm^{-1}{}^{\circ}C^{-1}$ for the basement rock in the survey area.

There are few heat-flow measurements reported for this study area. However in the Klamath Falls geothermal area, which borders this survey area to the north, an average of thirty-three heat flow determinations yielded the value 116 mW/m^2, with a range of 13 to 716 mW/m^2. A value of 12 mW/m^2 was found on the California-Oregon border at the northwest corner of Lower Klamath Lake. This suggests that hydrologic effects may control the heat-flow pattern at the north boundary of the survey area as it seems to near Klamath Falls by causing an extreme range of reported heat-flow values. Southeast of Lassen Peak at a point just outside of the survey area, a value of 80 mW/m^2 was determined.

Stacey (1977) gives a thermal conductivity of 2.5 $Wm^{-1}{}^{\circ}C^{-1}$ for igneous rocks, but <u>in situ</u> measurements for rocks characteristic of the

Grid location	North (512 grid) 40°41'-42°00' N lat 120°55'-122°38' W long		South (512 grid) 40°15'-41°34' N lat 120°45'-122°28' W long		NC1 (256 grid) 41°21'-42°00 N lat 121°53'-122°45' W long		NC2-W (256 grid) 41°21'-42°00' N lat 121°34'-122°26' W long		NC2 (256 grid) 41°21'-42°00' N lat 121°21'-122°13' W long		Medicine Lake(256 grid) 41°15'-41°54' N lat 121°12'-122°03' W long	
Grid size	146 km x 146 km		146 km x 146 km		73 km x 73 km		73 km x 73 km		73 km x 73 km		73 km x 73 km	
Mean terrain elevation ASL km	1.5		1.4		1.5		1.7		1.6		1.7	
Frequency of the spectral peak f_{max} in cycles/km	.007		.007-.014		.014		.030-.038		.030-.038		.030-.038	
	MINIMUM DEPTH TO SOURCE BOTTOM (5-km thick source)											
Source-depth km BFL	>25		18		>14		8		8		8	
km BSL	>22		15		>11		5		5		5	
	T_c=300°C	T_c=580°C	T_c=300°C	T_c=580°C	T_c=300°C	T_c=580°C	T_c=300°C	T_c=580°C	T_c=300°C	T_c=580°C	T_c=300°C	T_c=580°C
Vertical temp gradient °C/km	<13	<25	18	35	<24	<46	45	87	45	88	45	87
Surface heat flow* mW/m^2	<22	<42	31	60	<41	<79	77	148	77	149	77	148
	MAXIMUM DEPTH TO SOURCE BOTTOM (depth to source top controlled)											
Depth (km) BFL to source top	-		6.25 ± .45		-		2.73 ± .15		2.8 ± .1		3.0 ± .1	
Source bottom km BFL	-		31		-		10		9		9	
km BSL	-		28		-		7		6		6	
	T_c=300°C	T_c=580°C	T_c=300°C	T_c=580°C	T_c=300°C	T_c=580°C	T_c=300°C	T_c=580°C	T_c=300°C	T_c=580°C	T_c=300°C	T_c=580°C
Vertical temp gradient °C/km	-	-	10	20	-	-	35	67	39	76	39	75
Surface heat flow* mW/m^2	-	-	17	34	-	-	60	114	67	130	66	128

* Heat-flow values based on conductivity of 1.7 $Wm^{-1}°C^{-1}$, an average value for the Cascade Mountains.

Table 1. Estimated depths to Curie-point isotherm and/or magnetic source bottom from spectral analysis of aeromagnetic anomalies, and corresponding surface heat-flow and geothermal gradients.

(ASL - above sea level, BSL - below sea level, BFL - below flight level)

Grid location	NC3 (256 grid) 41°21'-42°00' N lat 120°50'-121°41' W long		NC4 (256 grid) 40°59'-41°38' N lat 121°53'-122°45' W long		NC5 (256 grid) 40°59'-41°38' N lat 121°21'-122°13' W long		NC6 (256 grid) 40°59'-41°38' N lat 120°50'-121°41' W long		NC7 (256 grid) 40°37'-41°16' N lat 121°45'-122°37' W long		NC8 (256 grid) 40°37'-41°16' N lat 121°15'-122°07' W long	
Grid size	73 km x 73 km		73 km x 73 km		73 km x 73 km		73 km x 73 km		73 km x 73 km		73 km x 73 km	
Mean terrain elevation ASL km	1.5		1.6		1.5		1.5		1.0		1.3	
Frequency of the spectral peak f_{max} in cycles/km	.021-.027		.014		.014		.014		.014		.014	
	MINIMUM DEPTH TO SOURCE BOTTOM (5km-thick source)											
Source bottom km BFL	9		>14		>14		>14		>14		>14	
km BSL	6		>11		>11		>11		>11		>11	
	T_c=300°C	T_c=580°C	T_c=300°C	T_c=580°C	T_c=300°C	T_c=580°C	T_c=300°C	T_c=580°C	T_c=300°C	T_c=580°C	T_c=300°C	T_c=580°C
Vertical temp gradient °C/km	40	77	<24	<46	<24	<46	<24	<46	<25	<48	<24	<47
Surface heat flow* mW/m^2	68	131	<41	<79	<41	<79	<41	<79	<43	<82	<41	<80
	MAXIMUM DEPTH TO SOURCE BOTTOM (depth to source top controlled)											
Depth (km) BFL to source top	3.24 ± .01		-		-		-		-		-	
Source bottom km BFL	15		-		-		-		-		-	
km BSL	12		-		-		-		-		-	
	T_c=300°C	T_c=580°C	T_c=300°C	T_c=580°C	T_c=300°C	T_c=580°C	T_c=300°C	T_c=580°C	T_c=300°C	T_c=580°C	T_c=300°C	T_c=580°C
Vertical temp gradient °C/km	22	43	-	-	-	-	-	-	-	-	-	-
Surface heat flow* mW/m^2	37	73	-	-	-	-	-	-	-	-	-	-

* Heat-flow values based on conductivity of 1.7 $Wm^{-1}°C^{-1}$, an average value for the Cascade Mountains.

Table 1 (cont.). Estimated depths to Curie-point isotherm and/or magnetic source bottom from spectral analysis of aeromagnetic anomalies, and corresponding surface heat-flow and geothermal gradients.

(ASL - above sea level, BSL - below sea level, BFL - below flight level)

Grid location	NC9-NW (256 grid) 40°48'-41°27' N lat 121°02'-121°54' W long		NC9 (256 grid) 40°37'-41°16' N lat 120°45'-121°37' W long		NC9-S (256 grid) 40°26'-41°05' N lat 120°45'-121°37' W long		NC10 (256 grid) 40°15'-40°54' N lat 121°45'-122°37' W long		NC11 (256 grid) 40°15'-40°54' N lat 121°15'-122°07' W long		NC12-W (256 grid) 40°15'-40°54' N lat 120°58'-121°50' W long	
Grid size	73 km x 73 km		73 km x 73 km		73 km x 73 km		73 km x 73 km		73 km x 73 km		73 km x 73 km	
Mean terrain elevation ASL km	1.4		1.5		1.6		0.6		1.5		1.7	
Frequency of the spectral peak f_{max} in cycles/km	.035-.049		.035-.049		.017		.014		.014		.017	
	MINIMUM DEPTH TO SOURCE BOTTOM (5 km-thick source)											
Source bottom km BFL	7		7		>12		>14		>14		>12	
km BSL	4		4		>9		>11		>11		>9	
	T_c=300°C	T_c=580°C	T_c=300°C	T_c=580°C	T_c=300°C	T_c=580°C	T_c=300°C	T_c=580°C	T_c=300°C	T_c=580°C	T_c=300°C	T_c=580°C
Vertical temp gradient °C/km	56	107	55	105	<28	<55	<26	<50	<24	<46	<28	<54
Surface heat flow* mW/m^2	95	182	94	179	<48	<93	<44	<85	<41	<79	<48	<92
	MAXIMUM DEPTH TO SOURCE BOTTOM (depth to source top controlled)											
Depth (km) BFL to source top	2.27 ± .18		1.91 ± .07		-		-		-		-	
Source bottom km BFL	8		9		-		-		-		-	
km BSL	5		6		-		-		-		-	
	T_c=300°C	T_c=580°C	T_c=300°C	T_c=580°C	T_c=300°C	T_c=580°C	T_c=300°C	T_c=580°C	T_c=300°C	T_c=580°C	T_c=300°C	T_c=580°C
Vertical temp gradient °C/km	47	91	40	77	-	-	-	-	-	-	-	-
Surface heat flow* mW/m^2	80	155	68	131	-	-	-	-	-	-	-	-

* Heat-flow values based on conductivity of $1.7 Wm^{-1}°C^{-1}$, an average value for the Cascade Mountains.

Table 1 (cont.). Estimated depths to Curie-point isotherm and/or magnetic source bottom from spectral analysis of aeromagnetic anomalies, and corresponding surface heat-flow and geothermal gradients.

(ASL - above sea level, BSL - below sea level, BFL - below flight level)

Grid location	NC12 (256 grid) 40°15'-40°54' N lat 120°45'-121°37' W long		Secret Spring Mtn, - Natl. Lava Beds Area (10 128 grids)		Mount Shasta Area (6 128 grids)		Eddys Mountain Area (2 128 grids)		Big Valley Mtns, Area (17 128 grids)		NE of Lassen Peak Area (14 128 grids)	
Grid size	73 km x 73 km		36 km x 36 km		36 km x 36 km		36 km x 36 km		36 km x 36 km		36 km x 36 km	
Mean terrain elevation ASL / km	1.7		1.5		1:8		1.8		1.2		1.7	
Frequency of the spectral peak f_{max} in cycles/km	.017		.033-.053		.033-.053		.034-.048		.035-.055		.033-.055	
	MINIMUM DEPTH TO SOURCE BOTTOM (5-km thick source)											
Source bottom km BFL	>12		6.9		6.4		6.9		6.8		6.4	
km BSL	>9		4.2		3.7		4.2		4.1		3.7	
	T_c=300°C	T_c=580°C	T_c=300°C	T_c=580°C	T_c=300°C	T_c=580°C	T_c=300°C	T_c=580°C	T_c=300°C	T_c=580°C	T_c=300°C	T_c=580°C
Vertical temp gradient °C/km	<28	<54	53	102	55	105	50	97	57	109	56	107
Surface heat flow* mW/m^2	<48	<92	90	173	94	179	85	165	97	185	95	182
	MAXIMUM DEPTH TO SOURCE BOTTOM (depth to source top controlled)											
Depth (km) BFL to source top	-		2.7 ± .6		1.9 ± .1		2.5 ± .1		2.3 ± .3		1.9 ± .2	
Source bottom km BFL	-		9.1		9.9		7.8		8.6		9.5	
km BSL	-		6.4		7.2		5.1		5.9		6.8	
	T_c=300°C	T_c=580°C	T_c=300°C	T_c=580°C	T_c=300°C	T_c=580°C	T_c=300°C	T_c=580°C	T_c=300°C	T_c=580°C	T_c=300°C	T_c=580°C
Vertical temp gradient °C/km	-	-	38	73	33	64	43	84	42	82	35	68
Surface heat flow* mW/m^2	-	-	65	124	56	109	73	143	71	139	60	116

* Heat-flow values based on conductivity of 1.7 $Wm^{-1}°C^{-1}$, an average value for the Cascade Mountains.

Table 1 (cont.). Estimated depths to Curie-point isotherm and/or magnetic source bottom from spectral analysis of aeromagnetic anomalies, and corresponding surface heat-flow and geothermal gradients.

(ASL - above sea level, BSL - below sea level, BFL - below flight level)

High Cascade Range in Oregon by Blackwell et al. (1978) suggest lower values. Heat-flow values listed in Table 1 are based on an average value of 1.7 $Wm^{-1}{}^{\circ}C^{-1}$ determined by Blackwell et al. (1978) for rocks from the western High Cascade Range. Using this single value seemed reasonable as the survey area is, for the most part, composed of the Cascade Range and associated Modoc Plateau. The value is also consistent with that used for the Cascade Range in a similar study concentrated in south-central Oregon (R. Couch and M. Gemperle, 1981, unpublished data).

A standard assumption in Curie-point depth analysis (Bhattacharyya and Leu, 1975; Shuey et al., 1977) is to use the Curie-point temperature of magnetite (Fe_3O_4), or 580°C. However, because titanomagnetite can lose its magnetization through low-temperature oxidation, a Curie-point temperature as low as 300°C is possible in the Earth's crust (Haggerty, 1978). The lack of heat-flow measurements in the survey area does not permit a choice of Curie-point temperature to be made.

Curie-point Depths

Figure 5 shows the magnetic-source depths, summarized in Table 1, superimposed on the topography. Figure 5 also shows calculated heat-flow values. These values are based on the magnetic-source-bottom depths, and on the assumption that these depths represent the depth of the Curie-point isotherm, that the Curie-point temperature is 580°C and that the conductivity is 1.7 $Wm^{-1}{}^{\circ}C^{-1}$. Survey markers locate the centers of 146 km x 146 km (512 x 512), 73 km x 73 km (256 x 256), and 36 km x 36 km (128 x 128) subgrids used in the analysis of anomalies in the study area. Thermal springs and wells with surface temperatures of $\leq$ 50°C or > 50°C, taken from a Geothermal Resources of California map (California Division of Mines and Geology, 1980), are indicated by triangles.

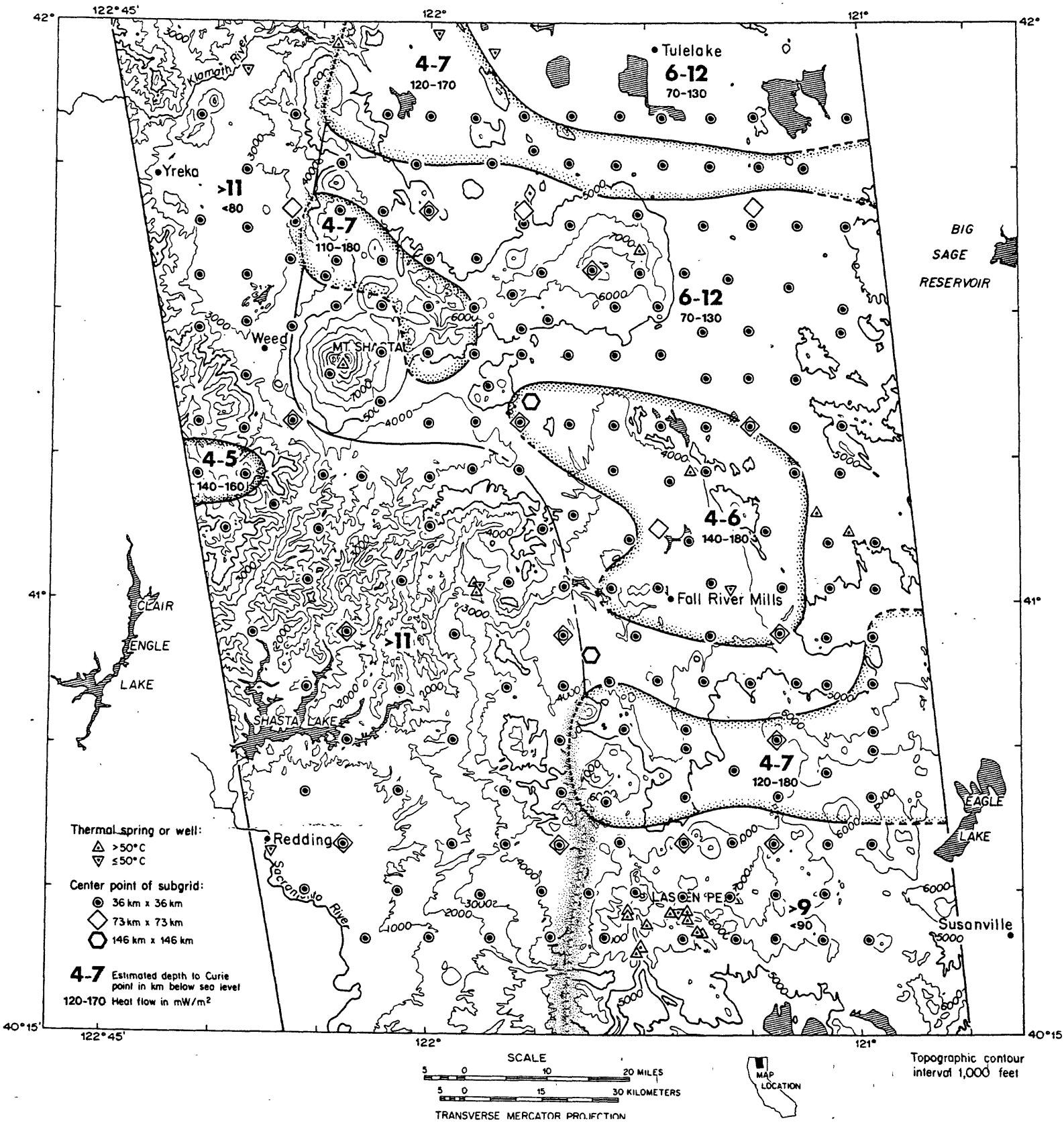

Figure 5. Estimated depth to the Curie-point isotherm and/or the depth to the bottom of the magnetic-source anomaly.

(Topographic base from U.S. Geological Survey maps NK 10-8, NK 10-9, NK 10-11, and NK 10-12.)

Analysis of several 36 km x 36 km sub-areas within the Secret Spring Mountain and National Lava Beds Monument area, the Mount Shasta area, the Eddys Mountains area, the Big Valley Mountains area, and northern part of the Lassen Peak area indicated extremely shallow magnetic-source and presumably Curie-point-isotherm depths.

The Secret Spring Mountain and National Lava Beds monument area is bounded on the north by the Mahogany Mountain Chain and the northern extent of the surficial lava beds, on the south by the Medicine Lake Highlands, and on the west by Shovel Creek. The elevated 'Curie-point' depth beneath this area, 4-7 km BSL (Below Sea Level), is the extension of an area of elevated Curie-point depths first mapped beneath the High Cascade Range north of this study area by McLain (1981). McLain (1981) gave 4-6 km BSL as the Curie-point-isotherm depth for this zone. The recent lava flows (Holocene) and reported thermal springs and wells located in the area also suggest elevated temperatures in the upper crust of the region.

A region of elevated 'Curie-point' depths (4-7 km BSL) lies beneath the Cascade Range near Mount Shasta. The region forms a quarter ring about Mount Shasta terminating immediately to the north and east of the mountain. Since Mount Shasta rises above the 9000-foot data-acquisition level, the reference level required for magnetic-source-depth determinations, the inner border of the ring is dashed in Figure 5 to indicate the zone could be enlarged. Thermal waters located at the summit of Mount Shasta supports this likelihood.

The elevated magnetic source depths (4-5 km BSL) beneath the area of the Eddys Mountain Range is bounded on the east by Mount Bradley, on the south by Castle Creek, and on the north by Mount Eddy. This area lies along the easternmost flank of the Klamath Mountains which

are composed of metamorphosed rocks of Mesozoic and Paleozoic age. It has been suggested (Couch and Gemperle, 1982) that magnetization in these rocks is induced, which, in turn, suggests that the magnetic source bottom resolved beneath the Eddys Mountains represents a lithologic boundary rather than the Curie-point isotherm depth.

The Big Valley Mountains area is bounded on the south by Bald Mountain, on the west by Buck Mountain and Lake Britton, on the north by the Medicine Lake Highlands, and on the east by Pit River. The elevated Curie-point depth beneath this region is 4-6 km BSL. This zone encompasses the Little Hot Spring Valley and a thermal spring located east of Fall River Mills. It lies to the east of the thermal springs located near Big Bend Mountain and lies to the west of the thermal springs located in Big Valley. Since the 36 km x 36 km (128 x 128) subgrids centered over the latter two thermal spring locations did not show spectral peaks, this implies the Curie-point depth is greater than 6 km BSL.

Elevated magnetic source depths (4-7 km BSL) are also mapped beneath an area immediately to the north and east of the Lassen Peak area. This region is bounded on the south by Prospect Peak, on the west by Burney Mountain, and on the north by Bald Mountain.

The shallow 'Curie-point' depths underlying Secret Spring Mountain and northern Mount Shasta areas represent a zone of elevated 'Curie-point' depths beneath the northern California High Cascade Range and an extension of a similar zone beneath the southern Oregon High Cascades discussed by McLain (1981) and beneath the central Oregon High studied by G. G. Connard, R. Couch, and M. Gimperle (1982, unpublished data). The segmented nature of this zone suggests that either discrete magma chambers are being observed under the northern California High Cascades or undulations in the Curie-isotherm surface are being discerned. The latter idea may

better explain the areas of elevated depths mapped beneath the southern extent of the Modoc Plateau, namely the Big Valley Mountains and northeast Lassen Peak areas, which both terminate along the High Cascades.

A 73 km x 73 km (256 x 256) subgrid centered over the Medicine Lake Highlands indicated the resolution of a magnetic-source bottom between 5-6 km BSL. However, 36 km x 36 km (128 x 128) subgrids centered over many locations in the area produced no spectral peaks. This suggests the magnetic-source-bottom depth beneath this area lies just beyond the depth range a 36 km x 36 km subgrid can resolve, namely 6 to 9 km.

Several 73 km x 73 km subgrids did not exhibit spectral peaks, although they include regions of mapped shallow magnetic-source-bottom depths. This may imply deeper source bodies beneath parts of the 256 x 256 subgrids which causes the spectral peaks to shift lower than the fundamental frequency. For this reason deeper source bodies (and hence deeper Curie depths) could underlie the Black Fox Mountain area southeast of Mount Shasta, the Egg Lake area northeast of the Big Valley Mountains, and the Blacks Mountain area southeast of Fall River Mills.

The 73 km x 73 km subgrid covering the northeast corner of the survey area and which stops at the California-Oregon border gives a source depth of 6-12 km. This value seems to agree with values of 6-13 km and 6-16 km reported by McLain (1981) for areas north of the border in Oregon.

Spectral analysis of magnetic anomalies along the west edge of the survey area which includes the western Cascade Mountains, and parts of the Klamath Mountains and Great Valley, indicates magnetic-source depths and hence Curie-point depths greater than 11 km BSL. Such a deep Curie-

point depth for the western Cascades appears consistent with low heat-flow values measured by Blackwell et al. (1978). For the Klamath Mountains, such a depth is indicative of old, highly metamorphosed rocks capable of only induced magnetization. Since the Great Valley is composed of a thick layer of sediments possibly overlying the southern extent of the Klamaths, a depth greater than 11 km BSL is reasonable for this area as well. It should also be noted that in this survey, the Curie-point isotherm depth indicated beneath the Klamath and Western Cascade Mountains in northern California is the same as that reported beneath the extension of these ranges into southern Oregon (McLain, 1981).

Although the Lassen Peak area comprising the southeast portion of the survey area contains much evidence for geothermal activity, i.e., Quaternary volcanoes, numerous thermal springs, and hydrogen-sulfide (H_2S) fumes, Curie-point isotherm depths were not resolved, i.e., no spectral peaks occurred in the analysis of 73 km x 73 km and 36 km x 36 km subgrids located in the region. A reason why the subgrids nearest Lassen Peak might fail to see a shallower magnetic source bottom where one may exist, is that the height of Lassen Peak prevented data collection at 9000 feet. This, in turn, may not have allowed a proper sampling of the frequencies necessary to produce a spectral peak. What was indicated from the 73 km x 73 km subgrids is a Curie-point depth greater than 9 km BSL, which is somewhat less than the depth (greater than 11 km BSL) indicated for the Great Valley region to the east.

Discussion

The calculated depths to the Curie-point isotherm in the Cascade Range in central Oregon (G. G. Connard, R. Couch, and M. Gemperle, 1982, unpublished data), in southern Oregon (McLain, 1981; R. Couch and M. Gemperle, 1981, unpublished data), and in northern Cali-

fornia (this report) and in the adjacent Basin and Range Province, when mapped, show two remarkable patterns: 1) The areas of minimum depth to the Curie-point do not necessarily coincide with the major centers of eruptive volcanism and 2) the areas of shallow Curie-point depths in the Basin and Range Province east of the Cascades and south of the Brothers Fault Zone show an elongation or banding that is oriented approximately east-west.

A thermal model of the Cascade Range based on the observed heat flow (e.g., Blackwell et al., 1978), on the depth and temperatures of the Curie-point isotherm reported here, and on conductive heat flow, would imply melt or partial melt at depths of less than one half the thickness of the Earth's crust as indicated by gravity (Dehlinger and others, 1968; Thiruvathukal and others, 1970) and seismic-refraction measurements (Hill and others, 1981).

Studies of compressional and shear-wave travel times (Dehlinger and others, 1965) and seismic-refraction measurements (Hill and others, 1981) indicate not only that crustal and mantle phases (P*, S*, P_n, ξ'Sn) pass beneath and along the Cascades but that a Moho is detectable beneath the Cascades.

These seemingly conflicting indications of the constitution of the crust and upper mantle beneath the Cascade Range suggest a thermal model that allows high temperatures at a shallow depth without raising the temperature of the lower crust and uppermost mantle above the melting temperature. We propose that the high upper crustal temperatures and thermal gradients are a consequence of the mass-transport of heat as

magma from the upper mantle to the upper crust along relatively small conduits. As the magma reaches the upper crust, structures, tectonically and/or petrologically derived, guide and constrain the surfaceward movement of the fluid. The magma is intruded along a band (i.e. the Cascade Range) as sills, dikes, plugs, and irregular bodies and extruded to form the more familiar surface features of the Cascade Range. The surface heat flow is then an integration of two factors: 1) the manifestations of intrusions and their thermal halos that are and have been highly variable in time and space and 2) the flow and circulation of meteoric water to depths of 4 to 5 km. This model suggests that the surface manifestations of high temperatures at depth (e.g. volcanoes, hot springs) are not necessarily over the shallow hot rocks as indicated by the Curie-point isotherm depths but may be significant distances from them. That is, in the upper crust, there may be as much lateral flow as vertical flow in the upward migration of magma as well as geothermal fluids.

The east-west elongation of the zones of shallow Curie-point isotherms in the Basin and Range Province is enigmatic. Speculative investigations might relate them to the same causal process as the eastward migration with time of the rhyolite intrusions described by MacLeod and others (1976) or the east-west patterns of the Cenozoic igneous rocks in Nevada and Utah described by Stewart and others (1977).

Acknowledgements

The work reported above has been realized through the efforts of personnel of the Geophysics Group, Oregon State University. John Bowers, Gerald Connard, and William McLain assisted in making the measurements and in the preliminary processing of the measurements. JoAnne Huppunen computed the depths to the Curie-point. Steve Troseth prepared the maps and illustrations and Donna Moore assisted in the preparation of the report.

This work was supported by the U.S. Geological Survey's Extramural Geothermal Research Program under Grant No. 14-08-0001-G-623.

References Cited

Bhattacharyya, B.K., 1966, Continuous spectrum of the total magnetic field anomaly due to a rectangular prismatic body: Geophysics, V. 31, p. 97-112.

Bhattacharyya, B.K., and Leu, L.K., 1975, Analysis of magnetic anomalies over Yellowstone National Park: mapping the Curie-point isotherm surface for geothermal reconnaissance: J. Geophys. Res., v. 80, p. 4461-4465.

Blackwell, D.D., Hull, D.A., Bowen, R.G., and Steele, J.L., 1978, Heat Flow of Oregon: Oregon Dept. of Geological and Mineral Industry Special Paper 4, 47 p.

Boler, F.M., 1978, Aeromagnetic measurements, magnetic source depths, and the Curie-point isotherm in the Vale-Owyhee, Oregon geothermal area: M.S. Thesis, Oregon State University, Corvallis.

Briggs, I.C., 1975, A program to contour using minimum curvature: Australia Bureau of Mineral Resources, Geology and Geophysics, Department of Energy and Minerals, report 1975/98.

California Division of Mines and Geology, 1980, Geothermal Resources of California: Geologic Data Map No. 4, 1:750,000.

Connard, G.G., 1979, Analysis of aeromagnetic measurements from the central Oregon Cascades: M.S. Thesis, Oregon State University, Corvallis.

Couch, Richard, and Gemperle, Michael, 1982, Aeromagnetic measurements in the Cascade Range and Modoc Plateau of northern California - Report on work done from June 1, 1980, to November 30, 1980: U.S. Geological Survey Open-File Report 82-932, 23 p.

Dehlinger, P., Chiburis, E.F., and Collver, M.M., 1965, Local traveltime curves and their geologic implications for the Pacific Northwest states: Seismol. Soc. Am. Bull., v. 55, p. 587-607.

Dehlinger, P., Couch, R., and Gemperle, M., 1968, Continental and oceanic structure from the Oregon coast westward across the Juan de Fuca Ridge: Can. Jour. of Earth Sci., v. 5, p. 1079-1090.

Haggarty, S.E., 1978, Mineralogical constraints on Curie isotherms in deep crustal magnetic bodies: Geophys. Res. Letters, v. 5, p. 105-108.

Hill, D.P., Mooney, W.D., Fuis, G.S. and Healy, J.H., 1981, Evidence on the structure and tectonic environment of the volcanoes in the Cascade Range, Oregon and Washington from seismic refraction/reflection measurements: (Abstract) Soc. EP. Geophy. Fifty-first Ann. Meet., Los Angeles, CA.

MacLeod, N.S., Walker, G.W., and McKee, E.H., 1976, Geothermal significance of eastward increase in age of upper Cenozoic rhyolitic domes in southwestern Oregon: Proc. 2nd United Nations Symp. on the Development and Use of Geothermal Resources, San Francisco, CA.

McLain, W.H., 1981, Geothermal and structural implications of magnetic anomalies observed over the southern Oregon Cascade mountains and adjoining Basin and Range Province: M.S. Thesis, Oregon State University, Corvallis, 150 p.

Pitts, G.S., 1979, Interpretation of gravity measurements made in the Cascade mountains and the adjoining Basin and Range Province in central Oregon: M.S. Thesis, Oregon State University, Corvallis.

Shuey, R.T., Schellinger, D.K., Tripp, A.C., and Alley, L.B., 1977, Curie depth determination from aeromagnetic spectra: Geophys. J.R. Astr. Soc., v. 50, p. 75-102.

Smith. R.B., Shuey, R.T., Freidline, R.O., Otis, R.M., and Alley, L.B., 1974, Yellowstone hot spot: new magnetic and seismic evidence: Geology, v. 2, p. 451-455.

Spector, A., 1968, Spectral analysis of aeromagnetic data: Ph.D. Diss., University of Toronto, Canada.

Spector, A., and Grant, F.S., 1970, Statistical models for interpreting aeromagnetic data: Geophysics, v. 35, p. 293-302.

Stacey, F.D., 1977, Physics of the Earth: John Wiley and Sons, New York, N.Y., 2nd ed., 414 p.

Steward, J.H., Moore, W.J., and Zietz, I., 1977, E-W patterns of Cenozoic igneous rocks, aeromagnetic anomalies and mineral deposits, Nevada and Utah: Geol. Soc. Am. Bull., v. 88, p. 67-77.

Thiruvathukal, J., 1968, Regional gravity of Oregon: Ph.D. Dissertation, Oregon State University, Corvallis, Oregon, 92 p.

Thiruvathukal, J., Berg, J.W. Jr., and Heinrichs, D.F., 1970, Regional gravity of Oregon: Geol. Soc. Am. Bull., v. 81, p. 725-738.